NUMERICAL ANALYSIS OF MEMORY EFFECT IN CAPUTO FRACTIONAL COOLING MODELS VIA EULER TYPE METHODS

Ylldrita SALIHI[1*], Krutan RASIMI[1], Vjollca SHEMSHI[2], Nexhibe SEJFULI RAMADANI[2]

[1]*Department of Mathematics, Faculty of Natural Sciences and Mathematics, North Macedonia*
[2]*Department of Informatics, Faculty of Natural Sciences and Mathematics, North Macedonia*
[*]*Corresponding author e-mail: yldrita.salihi@unite.edu.mk*

Abstract

Fractional differential equations have attracted significant attention due to their ability to model memory-dependent phenomena. In this paper, we study the numerical solution of a Caputo-type fractional differential equation using the L1 discretization scheme, comparing the explicit Forward Euler and implicit Backward Euler methods in terms of accuracy and stability.
The problem is studied on [0,5] with y(0)=0, using an interactive analysis to visualize and assess accuracy against the exact solution. A systematic analysis is performed for different discretization step sizes $h=0.1,\ h=0.01,\ h=0.001$ and fractional orders $\alpha=0.8,\ 0.9,\ 0.999$. The visualization is carried out separately for varying α with fixed step size *h*, and, conversely, with step size varied at fixed α, to analyze the memory effect. The maximum error is presented in a log–log plot, while the Caputo L1 weights (Euler weights) are analyzed to illustrate the memory effect**,** summarized in tables for comparison and stability analysis of the solution.
The comparison shows that the implicit Backward Euler method performs better in terms of stability and accuracy, especially when larger step sizes are used. Overall, the numerical results obtained in *Mathematica* suggest that implicit time-discretization methods are a reliable and robust choice for solving fractional differential equations, particularly when stability is important.

Keywords: Fractional differential equations; Caputo fractional derivative; L1 discretization scheme; Forward & Backward Euler method; stability, convergence & error analysis; memory effect.

Introduction

The fractional cooling model extends classical heat transfer to describe non-local and history-dependent processes. Based on fractional calculus, it has been applied to diffusion and heat transfer, introducing the concept of anomalous diffusion. More recently, it has been used to capture memory effects in complex materials where classical integer-order models are insufficient (Diethelm, 2010, Kilbas et al., 2006). A concrete example arises in biological tissues during thermal therapies, where temperature evolution depends not only on the current heat input, but also on the previous thermal exposure. Similarly, in composite engineering materials and heat-storage systems, memory effects influence how energy is absorbed and released over time. Fractional models therefore provide a more realistic framework for describing these processes.
The memory effect is directly related to the fractional order α. When $\alpha\to 1$, the model approaches the classical integer-order cooling law, where memory effects are weak and the system behaves locally in time. For smaller values of α, the influence of past states becomes stronger, meaning that the system retains a longer thermal memory. Thus, the fractional order controls the strength of memory and determines how strongly the history of the process affects the present dynamics (Podlubny, 1999).
Definition 1.1. (Riemann–Liouville Fractional Integral) (Diethelm, 2010, Podlubny, 1999) Let $f(t)$ be continuous on $(0,T]$ and $\alpha\in(0,1]$. The Riemann–Liouville fractional integral of order α is defined as

$$I^{\alpha} f(t) = \frac{1}{\Gamma(\alpha)} \int_0^t (t-\tau)^{\alpha-1} f(\tau) d\tau . \quad (1.1)$$

Definition 1.2. (Caputo Fractional Derivative) (Diethelm, 2010, Kilbas et al., 2006) Let $f(t)$ be continuous on $(0,T]$ and $\alpha \in (0,1]$. The Caputo fractional derivative of order α is defined as

$$D_t^{\alpha} f(t) = \frac{1}{\Gamma(1-\alpha)} \int_0^t (t-\tau)^{-\nu} f'(\tau) d\tau . \quad (1.2)$$

Definition 1.3. (Initial Value Problem) (Podlubny, 1999) The initial value problem for $\alpha \in (0,1]$ and $t \in (0,T]$ is defined as

$$D^{\alpha} y(t) = f(t, y(t)),\ y(0) = y_0 . \quad (1.3)$$

Cooling Model

Based on this formulation, the fractional cooling model is introduced by defining the function according to a Newton-type cooling law that includes memory effects. At time *t*, a body's temperature $T(t)$ change is proportional to the difference between its temperature and the surrounding medium $T_m(t)$. Newton's law of cooling is typically modeled as a first-order initial value problem (Diethelm, 2010), however, real heat transfer processes in complex materials often exhibit memory effect and non-local behavior, that cannot be captured by classical derivative (Kilbas et al., 2006). To account for these hereditary effects, the classical derivative is replaced by the Caputo fractional derivative of order $\alpha \in (0,1)$, leading to the fractional cooling model (2.1).

Definition 2.1. (Fractional Cooling Model) The fractional cooling model of order α is given by

$$D_t^{\alpha} T(t) = -k\left[T(t) - T_m(t)\right],\ T(0) = T_0,\ k > 0 \quad (2.1)$$

where $k > 0$ denotes the cooling coefficient and T_m is the ambient temperature.

The Caputo fractional derivative is particularly suitable for physical applications because it allows the use of standard initial conditions expressed in terms of integer-order derivatives. In addition, it introduces a power-law memory kernel, meaning that the present state of the system depends on its entire thermal history (Podlubny, 1999). This memory effect reflects the fact that past temperatures continue to influence the current cooling dynamics, although their influence gradually decreases over time.

The fractional order α controls the strength of the memory effect. When $\alpha = 1$, the model reduces to the classical Newton cooling law and the system behaves locally in time. For $\alpha < 1$, the memory becomes stronger and the cooling process exhibits non-exponential behavior, which is commonly associated with anomalous diffusion phenomena (Garrappa, 2018). Such models are especially relevant in porous media, biological tissues, viscoelastic materials, and heterogeneous composite structures, where heat propagation deviates from classical diffusion laws (Sun and Wu, 2006, Garrappa, 2018). In biological tissue heating, for example, previous thermal exposure may continue to influence the present temperature distribution, making fractional models more realistic than classical approaches.

To validate the numerical schemes, a manufactured test problem is considered. The right-hand side of equation (1.3) is constructed so that the exact analytical solution is prescribed as $y(t) = t^2 - t$. Applying equation (1.2) and using the known fractional derivative formula, the forcing function is obtained analytically. This approach enables direct comparison between the

exact and numerical solutions and provides a reliable framework for analyzing the stability, convergence, and accuracy of the proposed numerical methods (Stynes, 2020).

Applying (1.2) to $y(t)$ and using $D_t^{\alpha} t^n = \frac{\Gamma(n+1)}{\Gamma(n+1-\alpha)} t^{n-\alpha}$, we obtain the forcing function:

$$f(t,\alpha) = \frac{2}{\Gamma(3-\alpha)} t^{2-\alpha} - \frac{1}{\Gamma(2-\alpha)} t^{1-\alpha} \qquad (2.2)$$

L1 discretization of Caputo derivative and numerical schemes

Let the interval $[0,1]$ be partitioned uniformly into N subintervals with step size $h = \frac{1}{N}$, defining the grid $t_n = nh,\ n = 0,1,...,N$. The L1 scheme approximated the Caputo derivative at t_n by replacing the integrand in Definition 1.2 with a piecewise linear interpolant of y at each $[t_k, t_{k+1}]$, leading into

$$D_t^{\alpha} y(t_n) = \frac{h^{-\alpha}}{\Gamma(2-\alpha)} \sum_{k=0}^{n-1} b_k \left(y_{n-k} - y_{n-k-1} \right),\ b_k = (k+1)^{1-\alpha} - k^{1-\alpha},\ b_0 = 1,\ k = 0,1,... \qquad (3.1)$$

The weights are strictly positive, monotonically decreasing to zero and satisfy the telescoping identity $\sum_{k=0}^{n-1} b_k = n^{1-\alpha}$. These properties ensure consistency of the approximation and reflect the fading memory property of (2.1), the influence of past values diminishes as $k \to \infty$ (Lin and Xu, 2007).

Fractional Euler Methods

The Euler method, in its various forms, is commonly used for ordinary differential equations and can be extended to fractional problems as (2.1) (Sun and Wu, 2006, Stynes, 2020).

Fractional Forward Euler Method (FEM): FEM employs a forward difference approximation for $D_t^{\alpha} y(t)$. The left-sided fractional rectangular formula is used to approximate the fractional derivative and is given by:

$$y_{n+1} = y_n + h f(t_n, y_n, \alpha),\ n = 0,1,...,N-1 \qquad (3.2)$$

The Fractional Backward Euler Method (BEM): BEM employs a backward difference approximation for $D_t^{\alpha} y(t)$. In this context, the right fractional rectangular formula provides a discrete approximation of the fractional derivative and can be written as follows:

$$y_{n+1} = y_n + h f(t_{n+1}, y_{n+1}, \alpha),\ n = 0,1,...,N-1 \qquad (3.3)$$

In formulas (3.2) and (3.3), the function f is obtained using (3.1).

Error and Convergence Analysis. Numerical Results

To assess the accuracy of the FEM and BEM, we compute the discrepancy between the numerical solution y_n and the exact solution $y(t) = t^2 - t$. Two error measures are employed, the maximum error and L2 error (normalized Euclidean norm) (Sun and Wu, 2006).

Definition 4.1. (Maximum Pointwise Error)

$$E_{\max} = \max \left\{ \left| y_n - y(t_n) \right| \middle| n = 1,2,...,N \right\} \qquad (4.1)$$

and captures the largest local deviation of the schemes over the entire interval $[0, 1]$.

Definition 4.2. (L_2 Error — Euclidean Norm)

$$E_{L2} = \|y_n - y(t_n)\| = \frac{1}{N}\sqrt{\sum_{n=1}^{N}\left(y_n - y(t_n)\right)^2} \tag{4.2}$$

reflects the overall global error of the method and is less sensitive to isolated local deviations. During the results, the convergence analysis is carried out by comparing the maximum error of FEM and BEM across three step sizes $h \in \{0.1, 0.01, 0.001\}$ with fixed fractional order $\alpha = 0.9$. The L1 approximation of the Caputo derivative is known to achieve a convergence order of $O\left(h^2\alpha\right)$ for a sufficiently smooth solution. According to $\alpha = 0.9$ the expected order is $O\left(h^{1.1}\right)$, while as $\alpha \to 1$ the convergence approaches the classical first-order rate. The convergence plot displays $E_{\max}$ as a function of h on a $\log-\log$ scale, allowing the convergence order to be estimated visually as the slope of the fitted line.

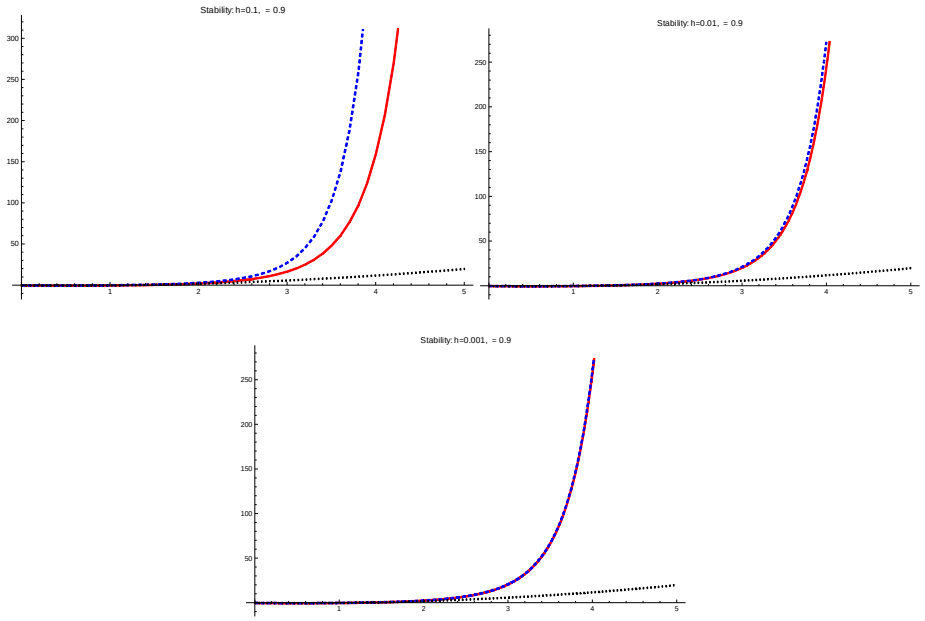

Figure 1. Stability analysis of (2.1) for $\alpha = 0.9$ and $h \in \{0.1, 0.01, 0.001\}$ using FEM (blue dashed line) and BEM(red solid line)

As illustrated in Figure 1, these features can be observed in the comparison between FEM (blue dashed line) and BEM (red solid line). Similar trends are also noted for other tested cases of α. In the following Figure 2, we observe the convergence of the methods through the maximum error and the log–log representation.

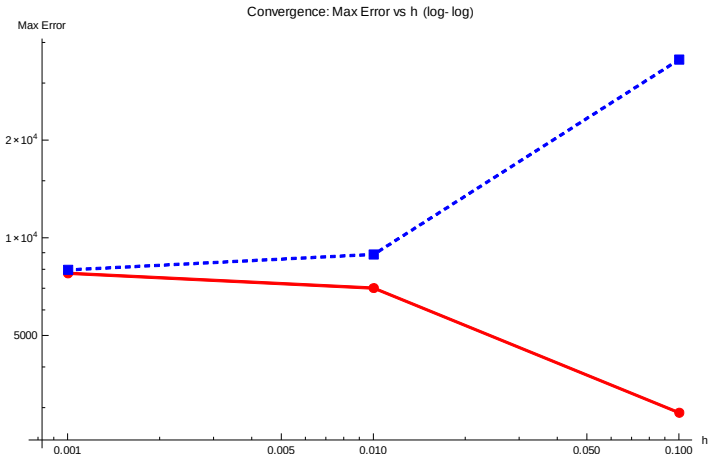

Figure 2. Maximum error (4.1) of FEM (red solid line) and BEM (blue dashed line) for $\alpha = 0.9$

Table 1. Maximum error (4.1) of FEM and BEM for a) $\alpha = 0.8$ *b)* $\alpha = 0.9$ *and c)* $\alpha = 0.999$

a)

H	FEM (E_{max})	BEM (E_{max})	FEM/BEM
0.1	2.82×10^3	3.451×10^4	8.17×10^{-2}
0.01	6.84×10^3	8.682×10^3	7.88×10^{-1}
0.001	7.596×10^3	7.779×10^3	9.76×10^{-1}

b)

H	FEM (E_{max})	BEM (E_{max})	FEM/BEM
0.1	2.9×10^3	3.554×10^4	8.16×10^{-2}
0.01	7.028×10^3	8.923×10^3	7.88×10^{-1}
0.001	7.805×10^3	7.993×10^3	9.76×10^{-1}

c)

H	FEM (E_{max})	BEM (E_{max})	FEM/BEM
0.1	2.967×10^3	3.64×10^4	8.15×10^{-2}
0.01	7.184×10^3	9.122×10^3	7.88×10^{-1}
0.001	7.976×10^3	8.169×10^3	9.76×10^{-1}

The results in Figure 2 and Table 1 demonstrate that both methods achieve convergence as the mesh parameter h decreases, with consistent behavior observed across the tested values of $\alpha \in \{0.8, 0.9, 0.999\}$. While BEM exhibits larger absolute maximum errors compared to FEM at coarse meshes (ratio of order 10^{-2}), the FEM/BEM ratio increases to approximately 10^{-1} as $h \to 0.001$, indicating that BEM converges at a relatively faster rate upon mesh refinement. Both methods display a clear monotone reduction in error as h decreases, confirming convergence across the entire range of tested fractional orders.

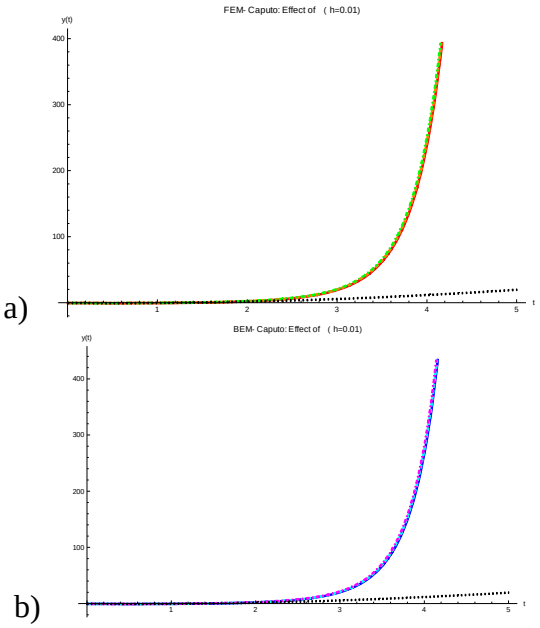

Figure 3. Effect of step size h for different values of α *for (2.1), a) FEM* $\alpha = 0.8,\ \alpha = 0.9,\ \alpha = 0.999$ *(red solid line, orange dashed line, green dashed point line, respectively); a) BEM* $\alpha = 0.8,\ \alpha = 0.9,\ \alpha = 0.999$ *(blue solid line, light blue dashed line, purple dashed point line, respectively)*

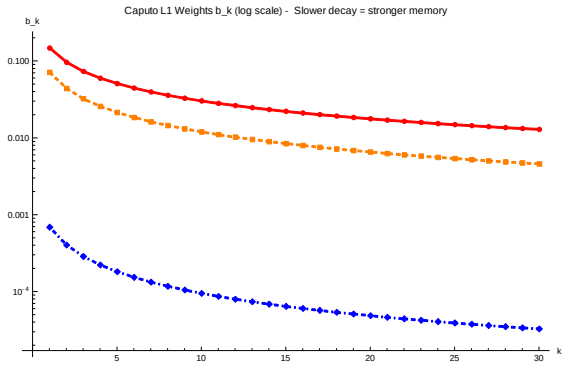

Figure 4. Caputo L1 weights b_k *,* $\alpha = 0.8,\ \alpha = 0.9,\ \alpha = 0.999$ *red, orange and blue respectively*

The weights are strictly positive, monotonically decreasing, and satisfy the telescoping identity, reflecting the inherent fading memory property of the Caputo fractional derivative. As $\alpha \to 1$, the weights decay more rapidly toward zero, indicating a diminishing influence of past values and a gradual transition toward classical integer-order dynamics.

Table 2 complements the analysis by reporting the L_2 errors, which capture the global approximation accuracy over the interval [0, 5]. The L_2 results confirm the trends observed in Table 1: the consistency between the pointwise and global error measures further validates the accuracy and stability of the proposed numerical framework.

Table 2. Maximum error (4.1) and L2 error (4.2) of FEM and BEM for a) $\alpha = 0.8$ b) $\alpha = 0.9$ and c) $\alpha = 0.999$

h	α	FEM L2	BEM L2	FEM (E_{max})	BEM (E_{max})
0.1	0.8	4.114×10^3	4.382×10^4	2.82×10^3	3.451×10^4
0.1	0.9	4.231×10^3	4.512×10^4	2.9×10^3	3.554×10^4
0.1	0.99	4.34×10^3	4.632×10^4	2.967×10^3	3.64×10^4
0.01	0.8	2.559×10^4	3.185×10^4	6.84×10^3	8.682×10^3
0.01	0.9	2.63×10^4	3.274×10^4	7.028×10^3	8.923×10^3
0.01	0.999	2.694×10^4	3.354×10^4	7.184×10^3	9.122×10^3
0.001	0.8	8.76×10^4	8.954×10^4	7.596×10^3	7.779×10^3
0.001	0.9	9.002×10^4	9.201×10^4	7.805×10^3	7.993×10^3
0.001	0.999	9.22×10^4	9.424×10^4	7.976×10^3	8.169×10^3

Caputo weights for $\alpha = 0.999$ and $k = 1,2,3,4,5$ are 0.000693387, 0.000405829, 0.00028804, 0.000223478, 0.000182632, $\alpha = 0.8$ and $k = 1,2,3,4,5$ are 0.148698, 0.0970326, 0.073777, 0.0602218, 0.0512394.

Figure 3 illustrates the sensitivity of the maximum error to the step size *h* for varying values of α. Both methods display a clear monotone reduction in error as *h* decreases, confirming convergence across the entire range of tested fractional orders. Figure 4. depicts the Caputo L1 weights b_k for $\alpha \in \{0.8, 0.9, 0.999\}$. The weights are strictly positive, monotonically decreasing and satisfy the telescoping identity, reflecting the inherent fading memory property of the Caputo fractional derivative. As $\alpha \to 1$, the weights decay more rapidly toward zero, indicating a diminishing influence of past values and gradual transition toward classical integer-order dynamics. Table 1 reports the maximum errors for both, FEM and BEM across all test values of α and *h*. At *h*=0.1, BEM yields substantially larger errors than FEM, with ratio s of the order 10^{-2}. However, as *h* is refined to 0.001, the FEM/BEM ratio increases to approximately 10^{-1}, indicating that BEM exhibits a faster convergence rate. This trend is consistent across all three values of α, demonstrating the robustness and reliability of both schemes.

Conclusions

In this paper, we presented a numerical comparison between the FEM and BEM for solving Caputo-type fractional cooling model on [0, 5]. The schemes were tested for fractional order $\alpha \in \{0.8, 0.9, 0.999\}$ and step size $h \in \{0.1, 0.01, 0.001\}$. Both methods achieve convergence consistent with the theoretical rate $O(h^{\alpha})$, with results recovering classical first-order behavior as $\alpha \to 1$. FEM provides better accuracy at coarser meshes, while BEM offers superior stability and faster convergence upon mesh refinement, confirming the advantage of implicit schemes for fractional problems. The results validate the effectiveness of L1-based discretization methods for Caputo fractional differential equations, supporting their use memory-dependent physical models. The analysis of the Caputo L1 weights also highlights the fading memory

property of the fractional derivative, showing how the influence of past states decreases over time depending on the fractional order. These results demonstrate the suitability of fractional models for describing memory-dependent thermal processes and other nonlocal physical phenomena.

Future Work

Future research may extend the proposed framework to nonlinear and variable-order fractional cooling models, as well as fractional delay differential equations. Incorporating time-delay effects would allow the model to capture delayed thermal responses and hereditary behavior more realistically.

Additional directions include adaptive time-stepping techniques and higher-order methods, such as predictor–corrector or fractional Adams schemes, to improve computational efficiency and accuracy. Applications to multidimensional heat transfer, biological tissues, and viscoelastic materials also remain topics for future investigation.

References

[1] Kai Diethelm. 2010. *The Analysis of Fractional Differential Equations*. Springer, Berlin.

[2] Igor Podlubny. 1999. *Fractional Differential Equations*. Academic Press, San Diego.

[3] Y. Lin and C. Xu. 2007. "Finite difference/spectral approximation for the time-fractional diffusion equation." Journal of Computational Physics, 225(2), 1533–1552.

[4] Z. Sun and X. Wu. 2006. "A fully discrete difference scheme for diffusion-wave system." Applied Numerical Mathematics, 56(2), 193–209.

[5] A. A. Kilbas, H. M. Srivastava and J. J. Trujillo. 2006. *Theory and Applications of Fractional Differential Equations*. Elsevier, Amsterdam.

[6] Martin Stynes. 2020. "Too much regularity may force too strong mesh refinement in fractional differential equation solvers." Computers & Mathematics with Applications, 80(1), 2247–2255.

[7] Roberto Garrappa. 2018. "Numerical Solution of Fractional Differential Equations: A Survey and Software Tutorial." Mathematics, 6(2), 16.

‘